Preparation of mesoporous activated carbon from date stones for the adsorption of Bemacid Red

Rabia Boudia, Goussem Mimanne, Karim Benhabib, Laurence Pirault-Roy

Preparation of mesoporous activated carbon from date stones for the adsorption of Bemacid Red

Rabia Boudia, Goussem Mimanne, Karim Benhabib and Laurence Pirault-Roy

Rabia Boudia, Goussem Mimanne (corresponding author)

Department of Chemistry, Materials and Catalysis Laboratory (LMC), BP89 University Dillali Liabes of Sidi Bel Abbes, 22000, Sidi Bel Abbes, Algeria,

E-mail: *g.mimanne@yahoo.fr*; *goussem.mimanne@univ-sba.dz*

Karim Benhabib

Eco-PRocédés Optimisation et Aide à la Décision (EPROAD, EA4669) Université de Picardie Jules Verne,
IUT de l'Aisne, 48 rue d'Ostende, 02100 Saint-Quentin, France

Laurence Pirault-Roy

Université de Poitiers, CNRS UMR 7285, Institut de Chimie des Milieux et Matériaux de Poitiers (IC2MP), 4 rue Michel Brunet, TSA 51106, 86073 Poitiers Cedex 9, France

ABSTRACT

This work concerns the elimination of the organic pollutant; Bemacid Red (BR), a rather persistent dye present in wastewater from the textile industry in western Algeria, by adsorption on carbon from an agricultural waste in the optimal conditions of the adsorption process. An active carbon was synthesized by treating an agro-alimentary waste, the date stones that are very abundant in Algeria, physically and chemically. Sample after activation (SAA) with phosphoric acid was highly efficient for the removal of BR. The characterization of this porous material has shown a specific surface area that exceeds 900 m^2/g with the presence of mesopores. The iodine value also indicates that the activated carbon obtained has a large micro porosity. The reduction of the infrared spectroscopy (FTIR) bands reveals that the waste has been synthesized and activated in good conditions. Parameters influencing the adsorption process have been studied and optimized, such as contact time, adsorbent mass, solution pH, initial dye concentration and temperature. The results show that for a contact time of 60 min, a mass of 0.5 g and at room temperature, the adsorption rate of the BR by the SAA is at its maximum. Pseudo-first-order, pseudo-second-order and intraparticle diffusion models were studied to analyse adsorption kinetics. The result shows the adsorption kinetic is best with the pseudo-second-order model. In this study, Langmuir, Freundlich and Temkin isotherms were investigated for adsorption of BR onto SAA. The Freundlich and Temkin isotherms have the highest correlations coefficients. The suggested adsorption process involves multilayer adsorption with the creation of chemical bonds. The mechanism of adsorption of BR by SAA is spontaneous and

exothermic, and the Gibbs free energy values confirm that the elimination of the textile dye follows a physisorption.

Key words: adsorption, agro-waste, Bemacid Red, date stones, dye

INTRODUCTION

Dyes from textile, leather, cosmetics, paper, dye synthesis, food processing, pharmaceuticals and plastics industries are the important source of environmental contamination (Yao *et al.* 2010).
Various methods have been studied to remove dyes from wastewaters, including chemical oxidation (Liu *et al.* 2011), biodegradation (Ong *et al.* 2005), electrocoagulation (Golder *et al.* 2005) and adsorption (Vargas *et al.* 2011). However, these methods have many disadvantages, as they require expensive equipment and/or a continuous need for chemicals (Malkoc *et al.* 2006). Moreover, sometimes the above-mentioned methods fail to meet the Environmental Protection Agency requirements (Borba *et al.* 2008; Baccar *et al.* 2009). Activated carbon is one of the most widely used adsorbents due to its high adsorbent power, but its cost and its regeneration are very expensive (Sudhakar *et al.* 2016). Appropriate agro-food waste (lignocellulosic), such as fishing and date cores, rice, pistachio and almond shells, have been studied in recent years as active carbon precursors and receive special attention (Baccar *et al.* 2009). The objective of this study is to develop an inexpensive adsorbent from date stones and explore the possibilityof using it to remove the dangerous dye Bemacid Red $C_{24}H_{20}ClN_4NaO_6S_2$ present in a wastewater by adsorption.

METHODS

Preparation of activated carbon

The amount of date stones was washed initially with hot water to remove impurities, dust, and water-soluble substances (Namane et al. 2005), and in a second step, distilled water was used to remove dirt and other contaminants and the stones were oven dried at 110 °C for 24 hours. Then, the sample was dried in an oven at about 200 °C for 3 hours. Finally, the stones were crushed and stored (SBA) before activation. 50 g of natural date stones were added to the aqueous solution of phosphoric acid (1/1) and stirred with heating to 100 °C for 1 hour. The sample was filtered and dried in an oven at 100 °C for 24 hours. Thereafter, the resulting sample was carbonized at a heating rate of 10 °C/min to 600 °C for 3 hours in a muffle furnace (NaberTherm B180).
After cooling, the carbonized sample was washed with an aqueous solution of hydrochloric acid (10% by weight) (Papirer et al. 1995) in order to remove the excess dehydrating agent and the soluble ash fraction, and then distilled water to remove residual organic and mineral matter. Washing with water easily removes most of the residues from activating agents (Namane et al. 2005). The sample was washed until the filtrate reached a neutral pH. The resulting sample was dried in an oven at 100 °C for 24 hours (SAA).

Characterization of the prepared adsorbent

Zero point charge pH (pH_{zpc})

The zero charge point (pHzpc) of the material was determined by the electrochemical method cited by Altenor (Altenor et al. 2009). A series of experiments was established by stirring 1 g of SAA in several solutions of distilled water at different pHs ranging from 2 to 12. The final pH was measured after 24 hours of stirring.

Iodine adsorption capacity

The iodine adsorption capacity of activated carbon prepared from date pits (SAA) was determined (Dhidan 2012). 10 mL of 0.01 N iodine solution was titrated with a 0.1 N sodium thiosulfate solution in the presence of a starch solution as an indicator until it became colourless. The reading volume corresponds to Vb.

0.05 g of SAA was mixed with 15 mL of an aqueous solution of iodine (0.1 N) and stirred vigorously for 5 min. The mixture was titrated with a standard sodium thiosulfate solution using a starch solution as an indicator, keeping the burette reading corresponding to Vs. The iodine number was then calculated by using the following equation:

$$I.N = \frac{(V_b - V_s).N\ (126.9)(15/10)}{M} \qquad (1)$$

I.N: iodine number ($mg.g^{-1}$)

V_b and V_S: volume of sodium thiosulfate solution required for blank and sample titrations respectively (mL).

N: normality of sodium thiosulfate solution ($mol.L^{-1}$)

126.9: atomic weight of iodine ($g.mol^{-1}$).

M: mass of SAA used (g).

Ash content

The ash content was determined by standard method (CEFIC 1986). 0.5 g of activated carbon, with an average particle size of 250 µm, was dried at 80 °C for 24 h and placed in previously weighed ceramic crucibles. The samples were heated in a muffle furnace at 650 °C for 3 h.

The crucibles were then cooled to room temperature and weighed. The ashing rate was calculated using the following equation:

$$Ash\ (\%) = \frac{(W_{m3} - W_{m2}).}{W_{m1}}\ x\ \ 100 \qquad (2)$$

where:
W_{m1}: weight of the original sample used (g);
W_{m2}: weight of crucible containing a dried sample (g);
W_{m3}: weight of crucible containing an original sample (g).

Moisture content

The moisture content was determined using the oven drying method (Adekola & Adegoke 2005). 0.5 g of activated carbon was placed in a previously weighed ceramic crucible.
The sample was dried at 110 °C until the weight was stable. Thereafter, the sample was cooled to room temperature and weighed. The moisture content was calculated using the following equation:

$$Moisture\ (\%)\ = \frac{(W_{m3} - W_{m2}).}{W_{m1}}\ x\ \ 100 \qquad (3)$$

Surface area (S_{BET})

The specific surface area of the SAA was evaluated by adsorption of N_2 at 77 K, using an ASAP 2010 V5.0. The BET model (Brunauer, Emmett and Teller) was applied. It consists of studying the nitrogen adsorption isotherm and evaluating the surface area (S_{BET}) of the sorbent.

FTIR analysis

The surface functional groups were studied by Fourier trans-form infrared spectroscopy (FTIR Perkin Elmer Universal ATR Sampling Accessory). The FTIR spectra of the raw material and the resulting activated carbon were recorded between 650 and 4,000 cm^{-1} in a Perkin Elmer spectrometer.

Adsorbate

Bemacid Red $C_{24}H_{20}ClN_4NaO_6S_2$, (M = 583 $g.mol^{-1}$) is anindustrial synthetic dye intended for the dyeing of chemical textiles of polyamide nature and which was supplied to us by a textile dyeing company in western Algeria. Bemacid Red (BR) belongs to group E, which is characterized by a high level of lightfastness, good migration power, good combinability, fast exhaustion even at low temperatures and rapid fixation with saturated steam. Bemacid Red is soluble in water and was used directly in the experiment without pre-treatment.

Adsorption study

A solution of 0.05 g. L^{-1} BR was prepared by dissolving an appropriate amount of dye, which was diluted to the required concentration. Various parameters that influence the adsorption process have been optimized. The optimal contact time was determined by stirring 1 g of SAA with 50 ml of a solution of BR 0.05 $g.L^{-1}$ at pH = 6 at times ranging from 5 to 90 min. The effect of the adsorbent dose was investigated by varying the amount of SAA from 0.1 to 0.6 g in 50 ml of 0.05 g. L^{-1} of dye solution

at pH = 6.

0.5 g of SAA was mixed with 50 ml of BR solution 0.05 g. L^{-1} at different pH values between 2 and 12 (the pH of the solution was adjusted using NaOH and HCl 0.1N) in order to study the effect of pH. To study the effect of the initial concentration of the BR dye, a mass of 0.5 g of SAA was mixed with 50 ml of the dye solution at different concentrations (0.01 to 0.07 g. L^{-1}). The effect of temperature on the adsorption phenomenon was studied by varying the temperature from 8 to 55 °C, maintaining the dye concentration at 0.05 g. L^{-1}, the time at 60 min, the mass of the adsorbent at 0.5 g and the pH of the solution at 2.

The dye concentration in the supernatant solution was determined at the characteristic wavelength BR λmax = 500 nm; by UV–visible spectrophotometer (Perkin Elmer UV-vis Lambda 45).

The percentage removal of the dye and the amount of dye adsorbed on the adsorbents (q_e) was calculated using Equations (4) and (5), respectively:

$$Removal\ (\%) = \frac{(C_0 - C_e).}{C_0} \times 100 \qquad (4)$$

$$q_e = \frac{(C_0 - C_e).V}{m} \qquad (5)$$

where:

q_e: amount of dye adsorbed on adsorbent at equilibrium ($mg.g^{-1}$);

C_0: initial equilibrium concentration of dye in solution ($mg.L^{-1}$);

C_e: equilibrium concentration of dye in solution ($mg.L^{-1}$);

V: volume of the solution (L);

m: mass of adsorbent (g).

Kinetics studies

Pseudo-first-order Equation (6), pseudo-second-order Equation (7) and intraparticle diffusion model Equation (8) were tested (McKay 1984; Ho & McKay 2000; Li et al. 2009).

$$\ln(q_e - q_t) = \ln\ q_e - k_1\, t \qquad (6)$$

$$\frac{t}{q_t} = \frac{t}{k_2 q_e^2} + \frac{t}{q_e} \qquad (7)$$

$$q_t = k_i\, t^{0.5} + C \qquad (8)$$

where:

q_e and q_t: adsorption capacity of the adsorbate ($mg.g^{-1}$) at equilibrium and at time t (min);

k_1 and k_2: pseudo-first-order and pseudo-second-order rate constant;

k_i: intraparticle diffusion rate constant;

C: the intercept.

Studies of adsorption isotherms models

The adsorbed amount of BR on SAA as a function of equilibrium concentration was determined as mixed 0.5 g of SAA with 50 ml of BR solution with various initial concentrations of 10, 20, 30, 40, 50, 60 and 70 mg.L^{-1} for 60 min, at pH = 2 and room temperature.

To determine the maximum BR capacity of SAA, the equilibrium isotherm data were correlated by the Langmuir (Clarke & Irving Langmuir 1916), Freundlich (Freundlich 1906; Haghseresht & Lu 1998), and Temkin (Sudhakar et al. 2016) isotherms. These equations can be written as Equations (9)–(11):

$$q = \frac{q_m K_L C_e}{1 + K_L C_e} \quad (9)$$

$$q = K_F C_e^{1/n} \quad (10)$$

$$q = \frac{q_m RT}{\Delta Q} \ln(K_T C_e) \quad (11)$$

where:

q_m : saturated adsorption capacity of the adsorbate (mg.g^{-1});

K_L: constant of Langmuir isotherm (L.mg^{-1});

K_F and n: parameters of the Freundlich isotherm;

K_T: Temkin constant (L.mol^{-1});

ΔQ: variation of adsorption energy (J.mol^{-1}).

Thermodynamic parameters

Gibbs free energy ΔG° (kJ.mol^{-1}), standard enthalpy ΔH° (kJ.mol^{-1}) and standard entropy ΔS° (J.mol^{-1}.K^{-1}) could provide information about the mechanism of adsorption and were determined using the van 't Hoff equation:

$$\Delta G^0 = -\mathrm{R\,T} \ln K_d \quad (12)$$

$$\Delta G^0 = \Delta H^0 - \mathrm{T}\,\Delta S^0 \quad (13)$$

$$\ln K_d = -\frac{\Delta H^0}{\mathrm{R\,T}} + \frac{\Delta S^0}{\mathrm{R}} \quad (14)$$

where:

R: universal gas constant (8.314 J.mol^{-1}.K^{-1});

T: absolute temperature (K);

K_d: thermodynamic distribution coefficient.

RESULTS AND DISCUSSION

Characterization of adsorbent

The adsorption isotherm (Figure 1) is divided into two parts: the first part (AB) has a slow increase of the convex curve and a large increase in the second part (BC) due to the multilayer adsorption, the filling, and the capillary condensation. In this case, no adsorption saturation point exists on the curve

(Wang et al. 2012). The shape of the curve shows a type IV adsorption-desorption isotherm according to the BDDT classification (Brunauer et al. 1940) with the presence of H3 hysteresis of the International Union of Pure and Applied Chemistry (IUPAC), which confirms the presence of mesopores (Song et al. 2009) in the form of a slit (Wang et al. 2012).

Hysteresis appeared at high relative pressure (p/p° > 0.6), suggesting that the synthesized material has a heterogeneous distribution of porous size (Li et al. 2007).

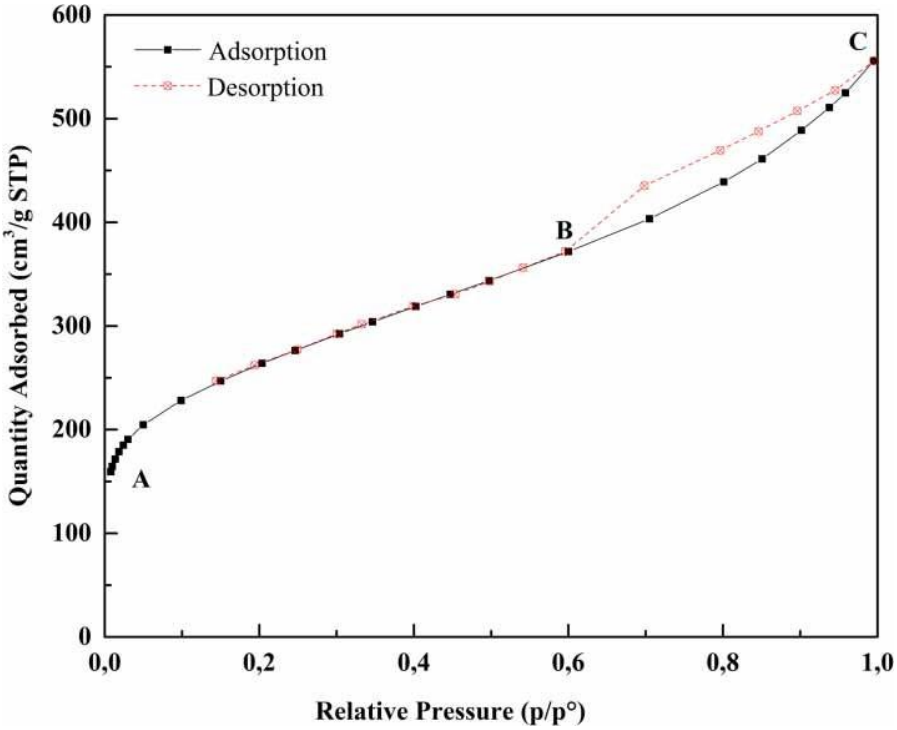

Figure 1 : N_2 adsorption-desorption isotherm of SAA.

The results obtained show that the SAA has a surface area equal to 942 $m^2.g^{-1}$, a pore volume of 0.504 cm^3/g and an average pore size of 2.14 nm. The average pore diameter of 2.14 nm indicates that the SAA is a mesoporous adsorbent according to the IUPAC classification.

Chemically activated carbon with H_3PO_4 shows a low pH_{pzc} value (2.59) (Figure 2), which indicates a high acidic group content (Altenor et al. 2009). The acidic or basic character of a surface is expressed by its isoelectric point. If the pH of the solution is basic, the surface is acidic and vice versa.

If $pH < pH_{pzc}$ then the net charge is positive

If $pH > pH_{pzc}$ then the net charge is negative

As the pH of the solution decreases to pH_{pzc}, the density of positive ions on the surface increases, causing strong attraction with BR that is negatively charged. Main chemical and textural properties of the activated carbons are listed in Table 1.

In addition, the pore characteristics such as surface area, total pore volume, and pore size of SAA at best conditions are 942 $m^2.g^{-1}$, 0.504 $cm^3.g^{-1}$, and 2.14 nm respectively. These values confirm the well developed pore structure of SAA compared to 1,080 $m^2.g^{-1}$, 0.622 $cm^3.g^{-1}$ and 2.850 nm for commercial activated carbon (CAC), respectively. The iodine number of SAA (1,142 mg. g^{-1}) is higher

than that obtained by Haimour and Emeish (Haimour & Emeish 2006). It should be emphasized that the optimum adsorption capacity of SAA iodine is slightly higher than that of a CAC, which has an iodine adsorption value of 1,000 mg . g^{-1} (Song et al. 2013). The contents of moisture and ash were 5.6 and 2.09% respectively. According to the results, the low ash content indicates that the precursor can withstand high temperature treatment during carbonization and chemical activation (Garba & Rahim 2016).

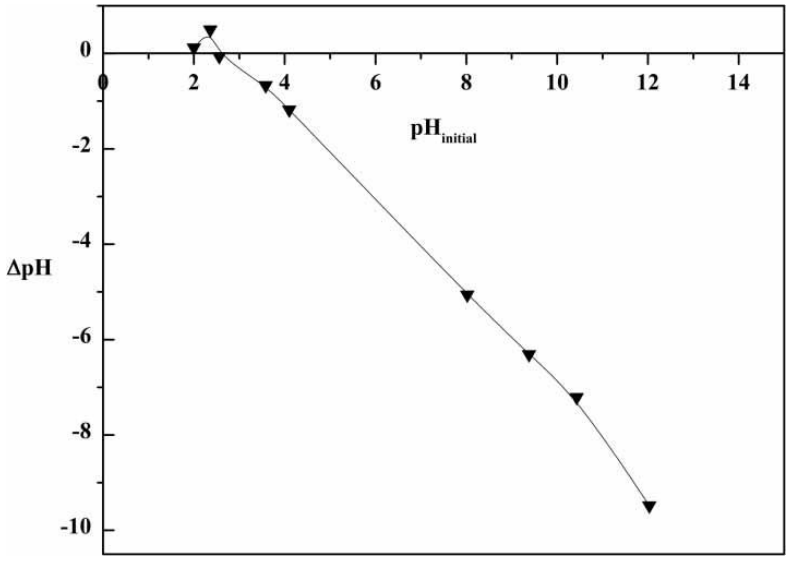

Figure 2 : Point of Zero Charge pH (pHpzc).

Table 1 : Chemical and textural properties of SAA

Characteristics	**Values**
Surface area(m^2 . g^{-1})	942
Pore volume (cm^3 .g^{-1})	0.504
Pore size (nm)	2.14
pHpzc	2.59
Iodine number (mg . g^{-1})	1,142
Ash content (%)	2.09
Moisture content (%)	5.6

Figure 3 shows the FTIR spectrum of the SBA (sample before activation) and SAA. The strong peaks, which appear at 3,685.8, 3,473.7 and 3,368.33 cm^{-1}, are attributed to bonded O-H groups (alcohols, phenols, and carboxylic acids) (Belala et al. 2011; Abbas & Ahmed 2016; El Messaoudi et al. 2016). The peaks between 2,989 cm^{-1} and 2,853 cm^{-1} correspond to the C-H (alkanes) (Abbas & Ahmed 2016; El Messaoudi et al. 2016). The peak at 1,744.08 cm^{-1} is characteristic of the stretching vibration of C=O of the carboxylic acids of xylan present in hemicelluloses (Sun et al. 2005; Pavan et al. 2008; El Messaoudi et al. 2016). Bands at 1,564.5 and 1,456.6 cm^{-1} attributed to the deformation C=C (aromatic of lignin) (Bouchelta et al. 2008; El Messaoudi et al. 2016). The vibration at 1,394.38,

1,376.4, 1,240.4 and 1,228.3 cm^{-1} attributed to the C-O methoxy groups of lignin (Al-ghouti et al. 2013; El Messaoudi et al. 2016). The band at 1,148.3 cm^{-1} corresponds to C-O (alcohols, carboxylic acids, ester, ethers) (Abbas & Ahmed 2016; El Messaoudi et al. 2016). Bands at around 1,064 cm^{-1} are attributed to the S-O elongation vibration (Kyzas et al. 2015; El Messaoudi et al. 2016). The peaks between 1,010 cm^{-1} and 936 cm^{-1} correspond to C-O-C bonds of cellulose (Sain & Panthapulakkal 2006; Al-ghouti et al. 2010; El Messaoudi et al. 2016). Peaks at 870,54 cm^{-1} and 880,1 cm^{-1} correspond to C-H deformation in cellulose (Sain & Panthapulakkal 2006; Al-ghouti et al. 2010; El Messaoudi et al. 2016). The band at 720,19 cm^{-1} is attributed to the C-X (alkyl halide) (Abbas & Ahmed 2016). The main groups present in the date stones before activation are the carbonyl and hydroxyl groups also found in the cellulosic biomass (Abbas & Ahmed 2016). Comparing the two FTIR spectra of SAA and SBA, we found that after activation various functions disappeared, such that: O-H, C=O, C-O-C, C-X.

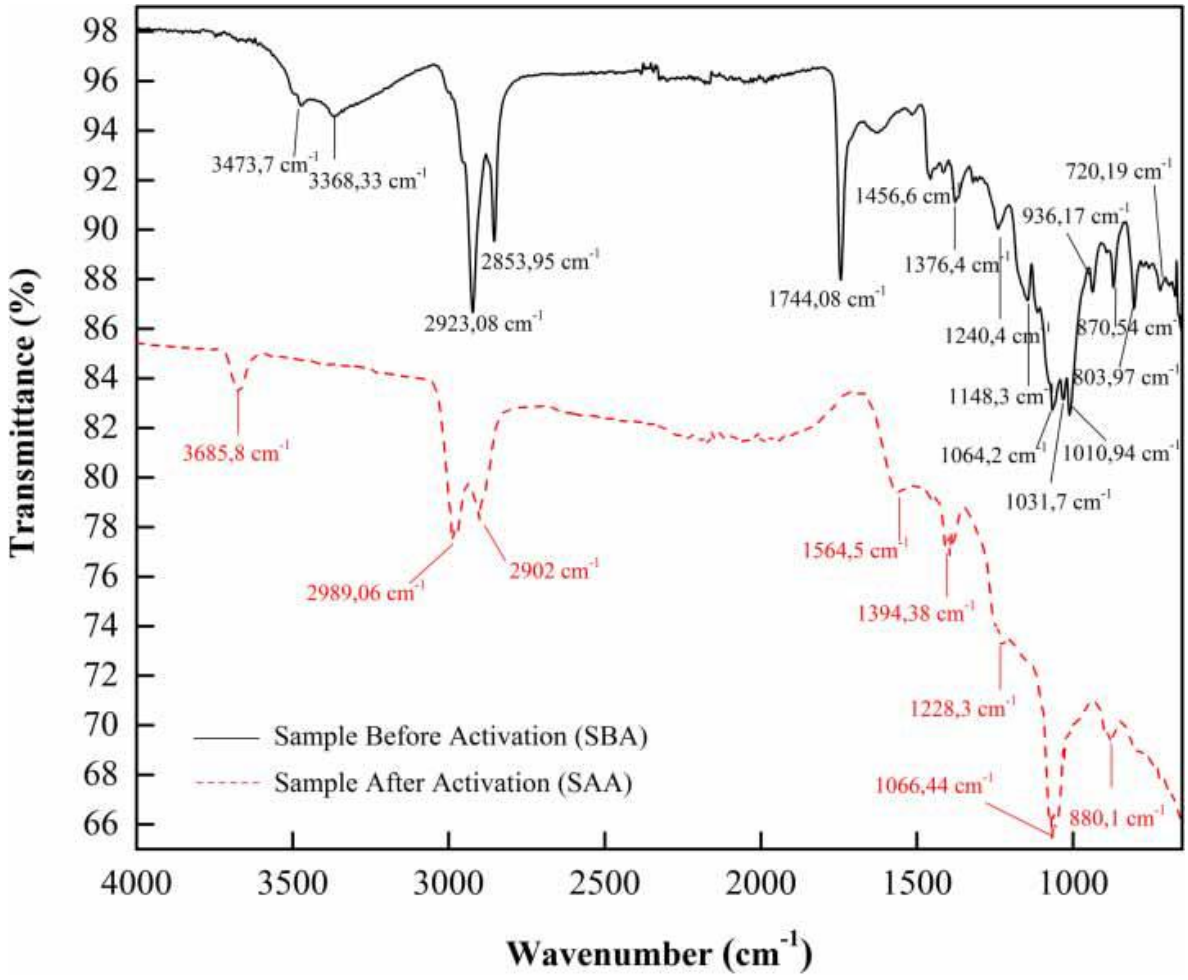

Figure 3: FTIR spectra of SBA and SAA.

Effect of contact time

Figure 4 shows a rapid increase in the elimination of the Bemacid Red with increasing contact time. Discoloration of the solution was observed from the first contact time (5 min). After a sufficient time

of 60 minutes, the residual concentration of the red dye in the aqueous phase reaches its limit.
The removal of BR (0.05 $g.L^{-1}$) is very fast at first contact, due to the availability of active sites. The adsorption rate becomes stable after 60 minutes of stirring and reaches equilibrium (Papirer et al. 1995). This equilibrium is due to the saturation of the majority of sites by dye ions.

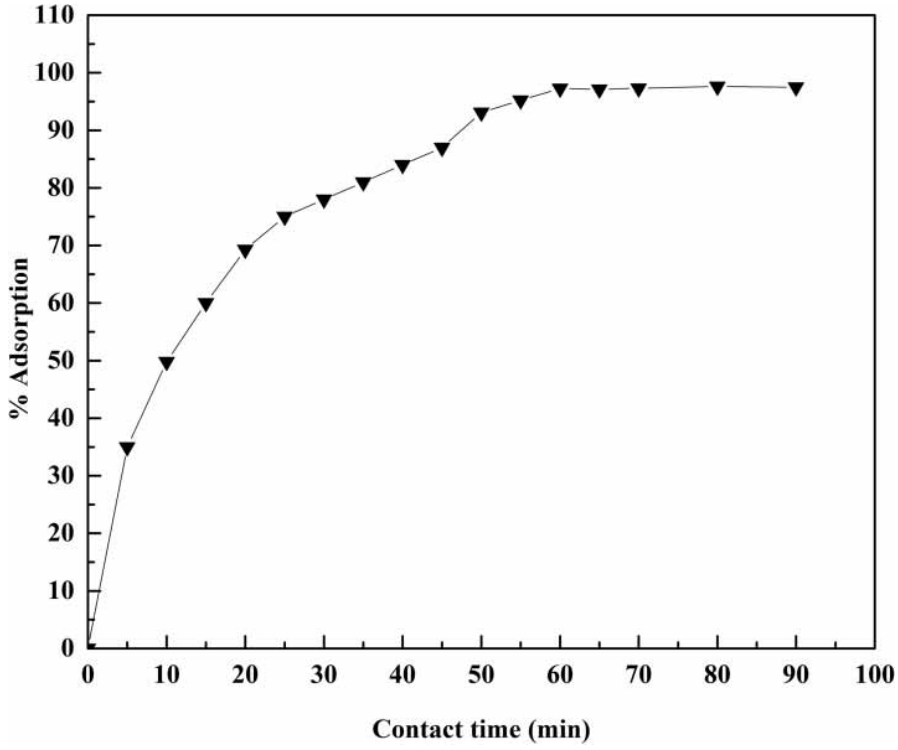

Figure 4 : Effect of contact time.

Effect of adsorbent amount

The effect of the adsorbent dose is investigated by varying the amount of SAA from 0.1 to 0.6 g in 50 mL of 0.05 $g.L^{-1}$ of BR dye solution. Figure 5 shows that with an increase in mass, the rate of BR adsorption increases from 25 to 95%. This is due to the presence of more active sites on the surface (Papirer et al. 1995; Kyzas et al. 2015). The initial increase in adsorption is due to the availability of a larger surface area of the adsorbent, but a further increase in the amount saturates the surface of the adsorbent and the equilibrium state is reached. The adsorption efficiency is reduced following the aggregation of the adsorption sites by an excess of adsorbent.

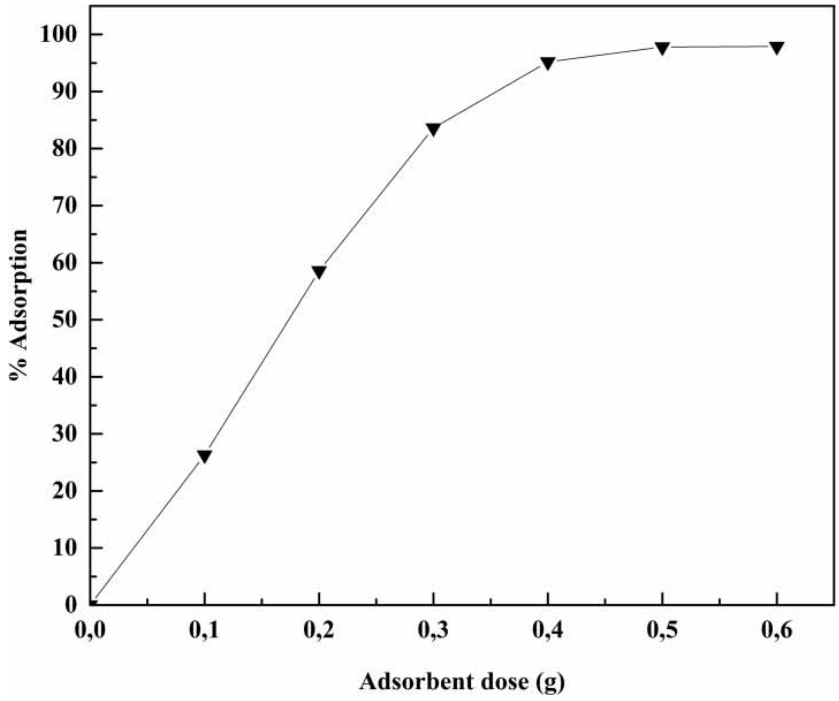

Figure 5: Effect of adsorbent dose

Effect of pH

0.5 g of SAA was mixed with 50 mL of BR solution at different pH values between 2 and 12 (the pH of the solution was adjusted using sodium hydroxide and nitric acid). Figure 6 shows the effect of the solution pH on the adsorption capacity of the SAA and it was found that the amount of adsorbed BR per unit of activated carbon increased significantly at a low pH.

SAA showed significant variation in percent removal from 99 to 66% on changing pH from 2 to 12. Maximum removal of SAA in an acidic medium may be due to the carboxylic and phenolic groups (cellulosic compounds) present on the adsorbent surface (Ferrero 2007). At low pH, the adsorption is at its maximum (at strongly acidic pH); this confirms the result obtained for the pHpzc. At pH< pHpzc, the surface is positively charged, which produces an attraction with the negatively charged pollutant.

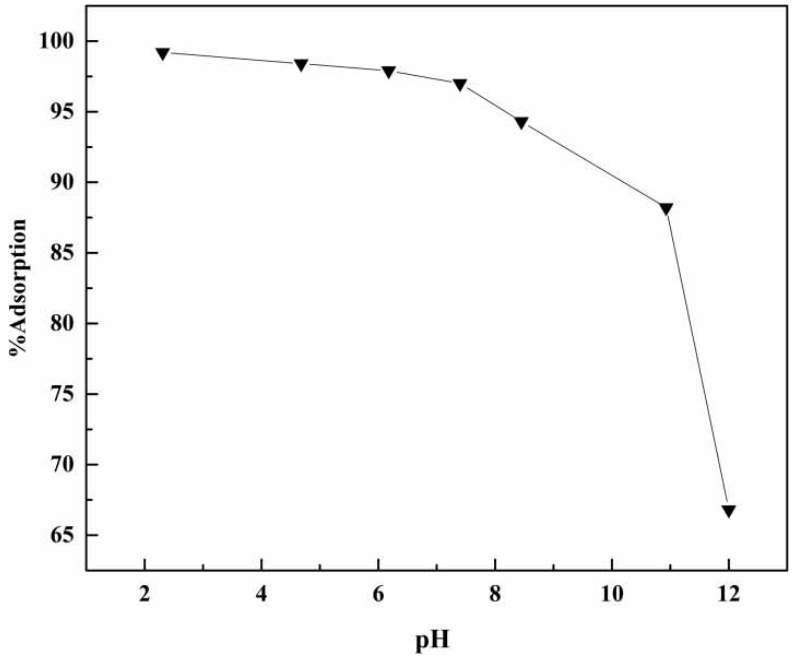

Figure 6 : Effect of pH.

Effect of initial concentration

Figure 7 shows that the adsorption rate was very fast at the first contact time and then gradually increased with time until the adsorption reached equilibrium. This rate of kinetics is due to the adsorption of the dye on the outer surface of the adsorbent at the beginning of the process.

When the adsorption on the outer surface reaches saturation, the dye diffuses into the pores of the adsorbent (adsorption on the inner surface of the adsorbent) (Kushwaha et al. 2014). The amount of BR adsorbed on SAA increased with increasing initial concentration. The initial concentration provides a driving force for overcoming the mass transfer resistance of dye molecules between the liquid and solid phases during adsorption (Ghaedi et al. 2014). This phenomenon can be explained by the fact that the initial high concentration of the dye provides a higher concentration gradient between the liquid phase and the solid phase, which increases the adsorption capacity (Maneerung et al. 2016).

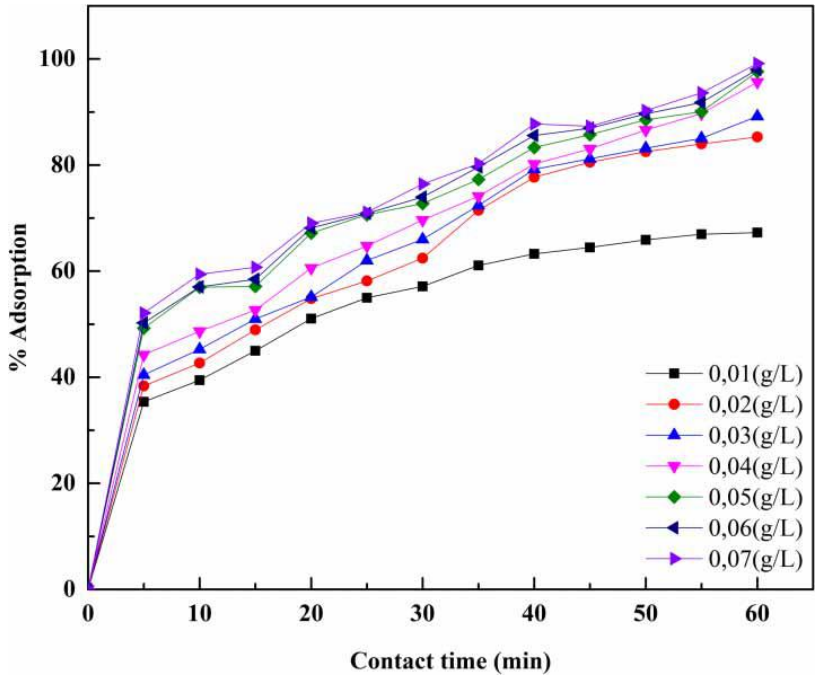

Figure 7 : Effect of initial concentration.

Effect of temperature

The effect of temperature on the adsorption phenomenon was studied by varying the temperature of the reaction medium from 8 to 55 °C (Figure 8).

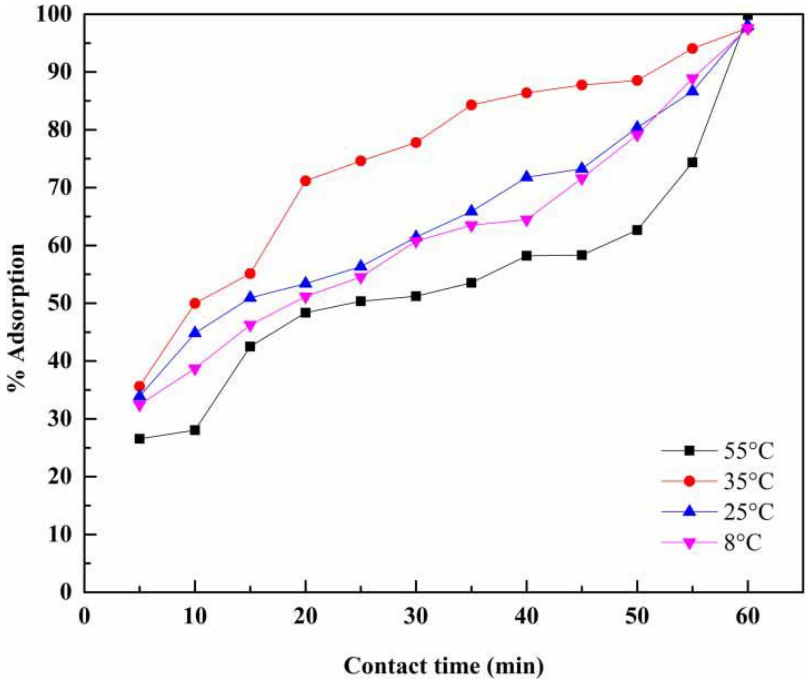

Figure 8 : Effect of temperature.

In the early stages, the percentages of elimination are almost identical for low temperatures. Beyond

5 minutes of stirring, this rate differs and the percentage of elimination reaches 90% for 35 °C, 85% for 8 °C and 25 °C and 70% for 55 °C. However, from 60 min, the adsorption rates increase for all temperatures and reach the same rate of elimination, which is 95%. Following these findings, it is best to work at room temperature.

Kinetic study

The value of the correlation coefficient R2 (Table 2) of the pseudo-second-order kinetic model, which is close to 1.0, and the value of the amount of equilibrium adsorbed dye (q_e), which is very close to that of the experimental value (1,320.25 mg . g^{-1}), indicate that the adsorption kinetics follow the pseudo-second-order model.

On the other hand, for the intraparticle diffusion model, the low value of R^2 for the linear plot of q_t versus $t^{1/2}$ indicates that this model could not properly fit the experimental kinetic data.

Table 2 : Kinetic parameters for adsorption of BR on SAA

		Results		
Kinetic models	*Constants*	*Ci= 30 mg.L^{-1}*	*Ci= 50 mg.L^{-1}*	*Ci= 70 mg.L^{-1}*
Pseudo first order	qe,cal (mg.g^{-1})	1758,11	1805,99	1956,23
	k_1 (mn^{-1})	7,28.10^{-3}	9,86.10^{-3}	11,23.10^{-3}
	R^2	0.92	0,9378	0,68
Pseudo second order	qe,cal (mg.g^{-1})	1270,33	1280,39	1300,54
	k_2 (mn^{-1})	1,63.10^{-3}	2,53.10^{-3}	2,48.10^{-3}
	R^2	0.99	0,9999	0,987
Intraparticle diffusion	q_e (mg.g^{-1})	1308,11	1511,03	1,450
	C	2,12	2,44	2,98
	k_i	1,12	1,25	1,32
	R^2	0,9321	0,9308	0,926

Adsorption isotherm study

From the values of the correlation coefficient (R^2) presented in Table 3, the BR adsorption process on SAA follows the Freundlich and Temkin models. The high value of n (>1) indicates a favorable adsorption. The constant n denotes the interaction between the exchange sites in the adsorbent and the BR ions. The Temkin model indicates that the adsorption mechanism between the dye and the sorbent is chemical, so the adsorption occurs at the most energetic sites in the beginning (Abdel-Ghani et al. 2007; Tiwari et al. 2015).

Table 3: R^2 and constants values for the different isotherm models

Models	Constants values
Freundlich	
R^2	**0.9904**
1/n	**0.211**
KF (mg . g^{-1})(L . mg^{-1})$^{1/n}$	**3.476**
Langmuir	
R^2	**0.86**
q_m (mg . g^{-1})	**5.017**
K_L (L. mg^{-1})	**1.0395**
Temkin	
R^2	**0,973**
B_T (kJ . mol^{-1})	**24.03**
K_T (L . mol^{-1})	**2.35**
ΔQ (J . mol^{-1})	**1.930**

Thermodynamic study

The effect of temperature on adsorption capacities was studied by performing a series of experiments at 281, 298, 308 and 328 K. Thermodynamic parameters such as enthalpy (ΔH°), entropy (ΔS°) and Gibbs free energy (ΔG°) were determined by Equations (7) and (8). The calculated values are given in Table 4.

Table 4: Thermodynamic parameter for adsorption of Bemacid Red by prepared carbon

T (K)	281	298	308	328
ΔH° (kJ.mol^{-1})	- 45.76			
ΔS° (kJ.K^{-1}.mol^{-1})	- 0.11			
ΔG° (kJ.mol^{-1})	- 1.49	- 9.20	- 9.90	- 10.60

The decrease in ΔG° values with increasing temperatures indicates that adsorption becomes less favorable at higher temperatures. Negative values of ΔG° indicate that the adsorption process is spontaneous. The negative value of ΔH° suggests that the BR adsorption process on SAA is exothermic (Chowdhury et al. 2011; Arampatzidou & Deliyanni 2016). The negative value of entropy can be attributed to the fact that the dye molecules lose their randomness when they are adsorbed on the surface of the activated carbon (Chowdhury et al. 2011; Foo & Hameed 2012). Gibbs free energy values (- 1.49 to - 10.60 kJ/mol) confirmed that the adsorption of BR by SAA is a physisorption (Chowdhury et al. 2011; Garba & Rahim 2016).

CONCLUSION

In this study, activated carbon from agro-food waste was successfully used in the removal of the textile dye BR. The adsorbent obtained after physical and chemical activation has a fairly large surface area with a predominant mesoporosity. The pH = 2 and the temperature 298 K gave the maximum adsorption rate with 0.5 g of adsorbent and a contact time of 60 min. The adsorption equilibrium is perfectly described by the Freundlich and Temkin isotherms, while the kinetics obey the pseudo-second-order model. Negative values of ΔG°, ΔH°, and ΔS indicate that the adsorption process is spontaneous and exothermic. The results confirm that the date stones have great potential to be transformed into high quality activated carbon. Date stone is an inexpensive material for the treatment of industrial wastewater. The SAA, after adsorption of BR, will be regenerated thermally by pyrolysis. The organic compounds adsorbed in the activated carbon will be destroyed by thermal effect.

ACKNOWLEDGEMENTS

The corresponding author would like to thank the entire team of PHC-MAGHREB 16MAG11.

REFERENCES

Abbas,A. F.&Ahmed, M. J. 2016, Mesoporous activated carbon from date stones (Phoenix dactylifera L.) by one-step microwave assisted K_2CO_3 pyrolysis. J. Water Process Eng. 9, 201–207.

Abdel-Ghani, N. T., Hefny, M. & El-Chaghaby, G. A. F. 2007, Removal of lead from aqueous solution using low cost sorbents. *Int. J. Environ. Sci. Technol.* 4, 67–73.

Adekola, F. & Adegoke, H. 2005 Adsorption of blue-dye on activated carbons produced from rice husk, coconut shell and coconut coirpith. *Ife J. Sci.* 7 (1), 151–157.

Al-ghouti, M. A., Li, J., Salamh, Y., Al-laqtah, N., Walker, G. & Ahmad, M. N. M. 2010 Adsorption mechanisms of removing heavy metals and dyes from aqueous solution using date pits solid adsorbent. *J. Hazard. Mater.* 176, 510–520.

Al-ghouti, M. A., Hawari, A. & Khraisheh, M. 2013 A solid-phase extractant based on microemulsion modified date pits for toxic pollutants. *J. En iron. Manage.* 130, 80–89.

Altenor, S., Carene, B., Emmanuel, E., Lambert, J., Ehrhardt, J. J. & Gaspard, S. 2009 Adsorption studies of methylene blue and phenol onto vetiver roots activated carbon prepared by chemical activation. *J. Hazard. Mater.* 165, 1029–1039.

Arampatzidou, A. C. & Deliyanni, E. A. 2016 Comparison of activation media and pyrolysis temperature for activated carbons development by pyrolysis of potato peels for effective adsorption of endocrine disruptor bisphenol-A. *J. Colloid Interface Sci.* 466, 101–112.

Baccar, R., Bouzid, J., Feki, M. & Montiel, A. 2009 Preparation of activated carbon from Tunisian olive-waste cakes and its application for adsorption of heavy metal ions. *J. Hazard. Mater.* 162, 1522–1529.

Belala, Z., Jeguirim, M., Belhachemi, M., Addoun, F. & Trouvé, G. 2011 Biosorption of basic dye from aqueous solutions by date stones and palm-trees waste: kinetic, equilibrium and thermodynamic

studies. *DES* 271, 80–87.

Borba, C. E., Silva, E. A. d., Fagundes-Klen, M. R., Kroumov, A. D. & Guirardello, R. 2008 Prediction of the copper (II) ions dynamic removal from a medium by using mathematical models with analytical solution. *J. Hazard. Mater.* 152, 366–372.

Bouchelta, C., Salah, M., Bertrand, O. & Bellat, J. 2008 Preparation and characterization of activated carbon from date stones by physical activation with steam. *J. Anal. Appl. Pyrolysis.* 82, 70–77.

Brunauer, S., Deming, L. S., Deming, W. E. & Teller, E. 1940 On a theory of the van der waals adsorption of gases. *J. Am. Chem. Soc.* 62, 1723–1732.

CEFIC 1986 Test-method-for-Activated-Carbon_86.pdf.

Chowdhury, S., Chakraborty, S. & Saha, P.2011 Biosorption of Basic Green 4 from aqueous solution by *Ananas comosus* (pineapple) leaf powder. *Colloids Surfaces B Biointerfaces* 84, 520–527.

Clarke, F. W. & Irving Langmuir, B. 1916 Constitution of solids and liquids. *J. Am. Chem. Soc.* 38, 2221–2295.

Dhidan, S. K. 2012 Removal of phenolic compounds from aqueous solutions by adsorption onto activated carbons prepared from date stones by chemical activation with $FeCl_3$. *Journal of Engineering* 18, 63–77.

El Messaoudi, N., El Khomri, M., Bentahar, S., Dbik, A., Lacherai, A. & Bakiz, B. 2016 Evaluation of performance of chemically treated date stones: application for the removal of cationic dyes from aqueous solutions. *J. Taiwan Inst. Chem. Eng.* 67, 244–253.

Ferrero, F. 2007 Dye removal by low cost adsorbents: hazelnut shells in comparison with wood sawdust. *J. Hazard. Mater.* 142, 144–152.

Foo, K. Y. & Hameed, B. H.2012 Coconut husk derived activated carbon via microwave induced activation: effects of activation agents, preparation parameters and adsorption performance. *Chem. Eng. J.* 184, 57–65.

Freundlich, H. 1906 Über die Adsorption in Lösungen. *Zeitschrift für Phys. Chemie* 57U, 385–470.

Garba, Z. N. & Rahim, A. A. 2016 Evaluation of optimal activated carbon from an agricultural waste for the removal of para- chlorophenol and 2,4-dichlorophenol, process safety and environmental protection. *Institution of Chemical Engineers.* 102, 54–63.

Ghaedi, M., Nasab, A. G., Khodadoust, S., Rajabi, M. & Azizian, S. 2014 Application of activated carbon as adsorbents for efficient removal of methylene blue: kinetics and equilibrium study. *J. Ind. Eng. Chem.* 20, 2317–2324.

Golder, A. K., Hridaya, N., Samanta, A. N. & Ray, S. 2005 Electrocoagulation of methylene blue and eosin yellowish using mild steel electrodes. *J. Hazard. Mater.* 127, 134–140.

Haghseresht, F. & Lu, G. Q. 1998 Adsorption characteristics of phenolic compounds onto coal-reject-derived adsorbents. *Energy & Fuels* 12, 1100–1107.

Haimour, N. M. & Emeish, S. 2006 Utilization of date stones for production of activated carbon using phosphoric acid. *Waste Manag.* 26, 651–660.

Ho, Y. S. & McKay, G. 2000 The kinetics of sorption of divalent metal ions onto sphagnum moss peat. *Water Res.* 34, 735–742.

Kushwaha, A. K., Gupta, N. & Chattopadhyaya, M. C. 2014 Removal of cationic methylene blue and malachite green dyes from aqueous solution by waste materials of *Daucus carota*. *J. Saudi Chem. Soc.* 18, 200–207.

Kyzas, G. Z., Siafaka, P. I., Bikiaris, D. N., Koukaras, E. N. & Froudakis, G. E. 2015 Journal of colloid and interface science alternative use of cross-linked polyallylamine (known as Sevelamer pharmaceutical compound) as biosorbent. *J. Colloid Interface Sci.* 442, 49–59.

Li, X., Li, Z., Xia, Q. & Xi, H. 2007 Effects of pore sizes of porous silica gels on desorption activation energy of water vapour. *Appl. Therm. Eng.* 27, 869–876.

Li, Y., Gao, B., Wu, T., Sun, D., Li, X., Wang, B. & Lu, F. 2009 Hexavalent chromium removal from aqueous solution by adsorption on aluminum magnesium mixed hydroxide. *Water Res.* 43, 3067–3075.

Liu, C., Xu, H., Li, H., Liu, L., Xu, L. & Ye, Z. 2011 Efficient degradation of methylene blue dye by catalytic oxidation using the $Na_8Nb_6O_{19}13H_2O/H_2O_2$ system. *Korean J. Chem. Eng.* 28, 1126–1132.

Malkoc, E., Nuhoglu, Y. & Dundar, M. 2006 Adsorption of chromium(VI) on pomace-an olive oil industry waste: batch and column studies. *J. Hazard. Mater.* 138, 142–151.

Maneerung, T., Liew, J., Dai, Y., Kawi, S., Chong, C. & Wang, C. H. 2016 Activated carbon derived from carbon residue from biomass gasification and its application for dye adsorption: kinetics, isotherms and thermodynamic studies. *Bioresour. Technol.* 200, 350–359.

McKay, G. 1984 The adsorption of basic dye onto silica from aqueous solution-solid diffusion model. *Chem. Eng. Sci.* 39,129–138.

Namane, A., Mekarzia, A., Benrachedi, K., Belhaneche-Bensemra, N. & Hellal, A. 2005 Determination of the adsorption capacity of activated carbon made from coffee grounds by chemical activation with $ZnCl_2$ and H_3PO_4. *J. Hazard. Mater.* 119, 189–194.

Ong, S. A., Toorisaka, E., Hirata, M. & Hano, T. 2005 Biodegradation of redox dye Methylene Blue by up-flow anaerobic sludge blanket reactor. *J. Hazard. Mater.* 124,88–94.

Papirer, E., Polania-Leon, A., Donnet, J. B. & Montagnon, P. 1995 Fixation of potassium aurocyanide on active carbons. *Carbon N. Y.* 33, 1331–1337.

Pavan, F. A., Lima, E. C., Dias, S. L. P. & Mazzocato, A. C. 2008 Methylene blue biosorption from aqueous solutions by yellow passion fruit waste. *J. Hazard. Mater.* 150, 703–712.

Sain, M. & Panthapulakkal, S. 2006 Bioprocess preparation of wheat straw fibers and their characterization. *Industrial Crops and Products.* 23, 1–8.

Song, C., Du, J., Zhao, J. & Feng, S. 2009 Hierarchical porous core-shell carbon nanoparticles. *Chem. Mater.* 21,1524–1530.

Song, M., Jin, B., Xiao, R., Yang, L., Wu, Y., Zhong, Z. & Huang, Y. 2013 The comparison of two activation techniques to prepare activated carbon from corn cob. *Biomass and Bioenergy* 48, 250–256.

Sudhakar, P., Mall, I. D. & Srivastava, V. C.2016 Adsorptive removal of bisphenol-A by rice husk ash and granular activated carbon – a comparative study. *Desalin. Water Treat.* 57, 12375–12384.

Sun, X. F., Xu, F., Sun, R. C., Fowler, P. & Baird, M. S. 2005 Characteristics of degraded cellulose obtained from steam- exploded wheat straw. *Carbohydrate Research* 340, 97–106.

Tiwari, D. P., Singh, S. K. & Sharma, N. 2015 Sorption of methylene blue on treated agricultural adsorbents: equilibrium and kinetic studies. *Appl. Water Sci.* 5, 81–88.

Vargas, A. M. M., Cazetta, A. L., Kunita, M. H., Silva, T. L. & Almeida, V. C. 2011 Adsorption of methylene blue on activated carbon produced from flamboyant pods (*Delonix regia*): study of adsorption isotherms and kinetic models. *Chem. Eng. J.* 168, 722–730.

Wang, W., Liu, P., Zhang, M., Hu, J. & Xing, F. 2012 The pore structure of phosphoaluminate cement. *Open J. Compos. Mater.* 02, 104–112.

Yao, Y., Xu, F., Chen, M., Xu, Z. & Zhu, Z. 2010 Adsorption behavior of methylene blue on carbon nanotubes. *Bioresour. Technol.* 101, 3040–3046.